Instrument background determination and red-side signal level investigation

M. Sauvage, K. Okumura, N. Billot

Document change record		
Version	Date	Changes
1.0	July 27, 2009	Release of the document

Reference documents			
Ref.	ID	Version	Title
RD1	SAp-PACS-MS-0616-06	1.0	FM Photometer Focal Plane Unit User's Manual
RD2	PICC-KL-RN-004	Draft 1	Flux estimates (in-orbit and OGSE)
RD3	SAp-PACS-MS-0680-08	1.0	Saturation limits for the PACS photometer
RD4	SAp-PACS-MS-0305	2.0	Backgrounds, noise and sensitivities
RD5	PICC-ME-TN-027	1.0	PACS spatial coordinates cheat-sheet
RD6	PICC-NHSC-TR-019	1.0	Photometer FOV analysis report: CoP data
RD7	PACS-KT-SP-002	3.0	HERSCHEL PACS FPU Design Specification

Contents

1 Introduction

This document was originally made to capture the different background measurements we have made in flight on the telescope. However we measured puzzling values of the flux falling on the red side of the photometer so we are now turning it into an exploration of the instrument background situation on the bolometer side. For the time being we simply list the different evidences we have that something is not as expected on the red side but no strict conclusion can be drawn yet.

Before going on, we list here a few information that needs to be understood to grasp what we are saying below.

1.1 Position of the detectors on the sky

Since it is not completely trivial, we recall here the position of the individual detector matrices on the sky. As indicated in RD1, the numbering of the photometer matrices (1 to 8 for the blue side, 9 and 10 for the red side) is inherited from the hardware and does not take into account the fact that, because of the dichroic mirror that separate the blue and red beams, the red detector produces a mirror image of the blue detector. Therefore, when projected in the sky, the matrices numbers are arranged as shown on Figure 1.1 (adapted from RD5).

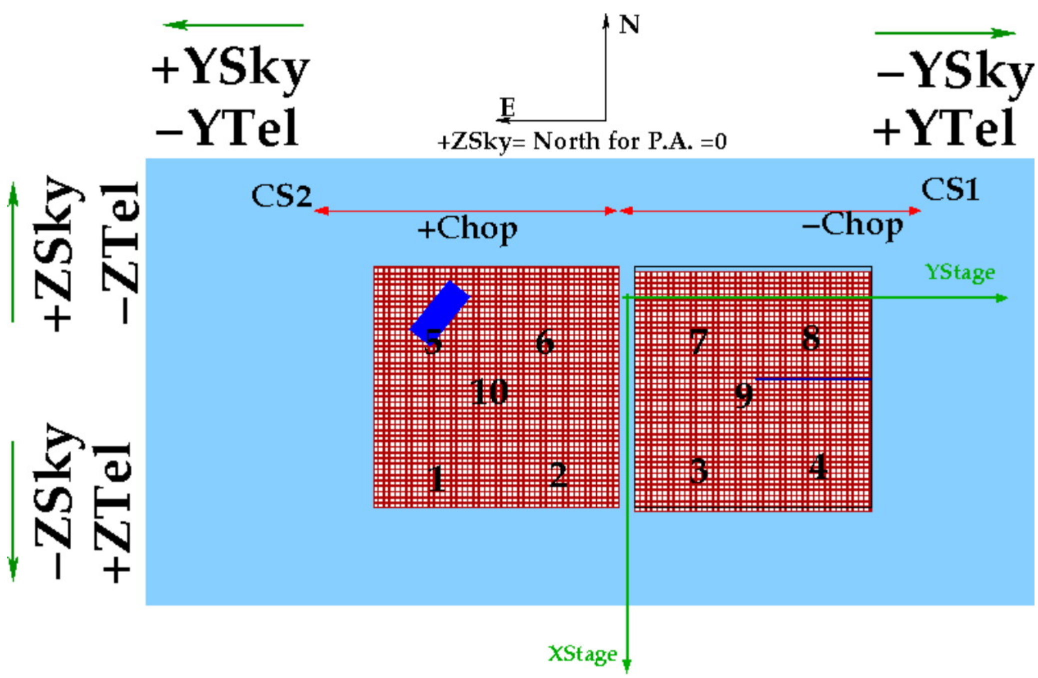

Figure 1: The PACS photometer field of view footprint on the sky. The numbers correspond to the matrices reference numbers used throughout this document, with the blue features outlining striking aspects of some arrays (missing line on array 8, group of bad pixels on array 10. This figure is adapted from RD5

.

The most important point to be made here is that **the red matrix 10 sees the same field of view as the blue matrices 1, 2, 5, and 6 while the red matrix 9 sees the same field of view as the blue matrices 3, 4, 7, and 8.**

1.2 Converting a measured signal into a flux level

This is a complex process involving “calibration” measurements coming either from flight or ILT tests (see also RD3 where this is explained in detail). The first step is to convert the signal recorded into the signal as measured at the middle point between the two bolometer resistors. This is done with the readout transfer function mapped in the `VRL-VH_BLIND` test and gives us V_{ptmil} which is independent from all bias set-up except the bolometer bias `VH-VL`. The transfer function has not changed since the FM-ILT. Expressing the signal in terms of V_{ptmil} allows much more straightforward comparison between different measurements than using either raw, or volt-converted raw data.

The second step is to convert this V_{ptmil} into a flux value and for that we rely on measurements made during the FM-ILT with the OGSE black-bodies. This conversion assumes that our computation of how much flux on a pixel corresponds to a given setting of the OGSE sources is correct. This computation was validated against flux estimates made in 2003 by M. Groenewegen. Given that the OGSE black-bodies required very different settings to provide a measurable flux on the blue or red side of the instrument, we have in fact two sets of measurement. One, referred to as B, is adapted to the blue side, i.e we record the V_{ptmil} values of all pixels for a range of blue fluxes from 1 to 7 pW/pix. In that same experiment we also get flux on the red side of the instrument so we record that data as well but the flux range is very different (around 20 pW/pix, i.e. much higher than the expected background range). The second set, R, is one where the flux range on the red side is set to 1 to 7 pW/pix, giving essentially 0 flux on the blue side.

1.3 Making a telescope background prediction

This is tricky. The only well-known part of the problem are the geometric parameters of the telescope, and the temperatures of the two mirrors (measured in flight simultaneously to the data we are using). Then there are other parameters never measured such as the transmission effect of the Lyot stop, estimated at 0.95, or a propagation efficiency parameter that tries and capture the effect of the secondary blocking some light, correction to the actual telescope surface (curved rather than flat), that we estimate at 1.04. These are however corrections of a few %.

Then we have to use an emissivity and for that we used the dusty mirror surface emissivity of Fischer et al. (2004, PASP 43, p3765).

Finally there is the stray light issue and this is completely open. We work on the assumption that the requirement given to industry is that it is not more than 30% of an hypothetical Herschel telescope with a 3% emissivity and mirrors at 70 K. With the above parameters for the telescope this gives in-band fluxes of $6.97\,10^{-1}$, $5.13 10^{-1}$, and 1.08 pW/pix in the blue, green, and red bands respectively.

Finally, we predict ranges of telescope backgrounds by allowing the emissivity and the stray light components to be multiplied by arbitrary factors. These are the largest source of variations in the telescope background prediction as the tables below show. The emissivity has its strongest impact at short wavelengths while the straylight influence is more important at long wavelengths.

2 Dedicated background measurements

In this section we analyse measurements that were meant to provide us with an assessment of the background level on a given day.

2.1 OD 32 - Pre-Preview - 1342178509

On OD 32 we prepared the sneak preview with a run of our 4 pre-determined settings on a random part of the sky (that in front of the telescope during DTCP). The first setting is the one that was least saturated so it can be used to estimate the background level on the instrument.

This measurement was performed on June 14, 13:35 UT. The M1 temperature was 116.34 K and the M2 temperature 111.29 K.

The prediction for these temperatures is listed in the following table:

M1 temperature:116.34 K, M2 temperature:111.29 K				
Emissivity factor	Stray light factor	Blue	Green flux (pW/pix)	Red
0.5	0.5	2.43	1.17	1.67
0.5	1.0	2.78	1.42	2.21
0.5	2.0	3.48	1.94	3.29
0.5	4.0	4.87	2.96	5.45
1.0	0.5	4.52	2.08	2.81
1.0	1.0	4.87	2.34	3.35
1.0	2.0	5.56	2.85	4.43
1.0	4.0	6.96	3.87	6.59
2.0	0.5	8.69	3.90	5.08
2.0	1.0	9.03	4.16	5.62
2.0	2.0	9.73	4.67	6.70
2.0	4.0	11.1	5.70	8.86
4.0	0.5	17.0	7.55	9.62
4.0	1.0	17.4	7.80	10.2
4.0	2.0	18.1	8.31	11.2
4.0	4.0	19.5	9.34	13.4

The computation of the background level, from the measured signal and using FM ILT calibrations is shown in the following tables. This gives a mean flux of 3.1 pW/pix in the blue filter, 2.0 pW/pix in the green filter and 4.4 pW/pix in the red filter.

1342178509 Blue					
VL	VH_BLIND	M5	M6	M7	M8
-0.198	1.995	3.058 ± 0.114	3.141 ± 0.134	3.396 ± 0.222	3.109 ± 0.109
VL	VH_BLIND	M1	M2	M3	M4
-0.198	1.995	2.91 ± 0.134	2.881 ± 0.085	3.068 ± 0.116	3.044 ± 0.104

1342178509 Red (from Blue obs.)			
VL	VH_BLIND	M9	M10
-0.23	2.016	4.323 ± 0.259	4.472 ± 0.393

1342178509 Green					
VL	VH_BLIND	M5	M6	M7	M8
-0.229	2.003	1.917 ± 0.086	1.985 ± 0.087	2.25 ± 0.171	1.997 ± 0.073
VL	VH_BLIND	M1	M2	M3	M4
-0.229	2.003	1.861 ± 0.113	1.827 ± 0.058	2.042 ± 0.097	2.038 ± 0.101

1342178509 Red (from Green obs.)			
VL	VH_BLIND	M9	M10
-0.23	2.016	4.344 ± 0.261	4.5 ± 0.397

Comparison of the measurement tables with the prediction values shows clearly that it is not simple to reconcile the telescope model with the observations: the blue and green data favor a telescope model with a rather low emissivity (half the prediction) and significant straylight (about twice the prescription), but the red data requires much more straylight (3-4 times the prescription). Though this is perfectly possible given the lack of knowledge on the straylight component, this is a first worrying sign.

Even more worrying is a comparison with a measurement made on that same day with the PACS spectrometer. Though to compare the two involves incorporating uncertainties coming both from the yet not fully calibrated spectrometer and from the photometer filter transmission curves, we expect 3.8 pW/pix in the blue filter, 1.9 pW/pix in the green filter, and 2.7 pW/pix on the red side. Thus we are roughly compatible for the green filter, slighly off for the blue filter and blattantly off for the red filter. We note however that is also hard to find a model of the telescope that is fine for all the spectrometer range.

2.2 OD 40 - Official First Background Measurement - 1342178914

The measurement was performed on June 23rd, 2009 at 3:41 UT. M1 temperature was 93.83K, M2 temperature was 90.73K. Predictions of the telescope flux with different contribution from the emissivity and the stray light are given below first for the same grid of emissivity and straylight factors as before, and then with a smaller emissivity factor and a higher straylight factor.

M1 temperature: 93.83 K, M2 temperature: 90.73 K				
Emissivity factor	Stray light factor	Blue	Green flux (pW/pix)	Red
0.5	0.5	1.62	0.869	1.36
0.5	1.0	1.97	1.13	1.90
0.5	2.0	2.67	1.64	2.98
0.5	4.0	4.06	2.66	5.14
1.0	0.5	2.89	1.48	2.18
1.0	1.0	3.24	1.74	2.72
1.0	2.0	3.94	2.25	3.80
1.0	4.0	5.33	3.28	5.96
2.0	0.5	5.44	2.70	3.83
2.0	1.0	5.78	2.96	4.37
2.0	2.0	6.48	3.47	5.45
2.0	4.0	7.88	4.50	7.61
4.0	0.5	10.5	5.15	7.11
4.0	1.0	10.9	5.41	7.65
4.0	2.0	11.6	5.92	8.73
4.0	4.0	13.0	6.95	10.9

M1 temperature: 93.83 K, M2 temperature: 90.73 K				
Emissivity factor	Stray light factor	Blue	Green flux (pW/pix)	Red
0.1	2.0	1.65	1.15	2.32
0.1	3.0	2.35	1.66	3.40
0.1	4.0	3.04	2.17	4.48
0.2	2.0	1.90	1.27	2.49
0.2	3.0	2.60	1.78	3.57
0.2	4.0	3.30	2.30	4.65
0.3	2.0	2.16	1.39	2.65
0.3	3.0	2.85	1.91	3.73
0.3	4.0	3.55	2.42	4.81

The long tables list the background levels measured on OD 40 with the so-called First Background measurement. The principle of the measurement is to explore a range of bias settings supposedly adapted to the predicted telescope background and check which of these settings leads to the smallest number of saturated pixels (hopefully 0). The purpose of the present report is not to fully analyse the observations in this context but rather to extract a value of the telescope background at that time. Since the background is not changing significantly during the measurement, we should obtain the same value for all matrices and all bias values for a given filter.

The tables below show the computation of the background values from the dedicated test. The flux values we compute are quite consistent with one another for the different settings used.

Taking the average values measured for the first setting we derive 1.8 pW/pix in the blue filter, 1.3 pW/pix in the green filter, and 4.0 pW/pix on the red filter. Once again we find ourselves in a situation where the blue and green filters observations can be explained with a telescope mode that has a very small emissivity and about twice as much straylight as predicted but the red filter requires significantly more straylight (about 4 times as much as predicted).

1342178914 Blue					
VL	VH_BLIND	M5	M6	M7	M8
-0.417	2.101	1.809 ± 0.109	1.891 ± 0.162	2.11 ± 0.251	1.826 ± 0.087
	2.201	1.798 ± 0.112	1.883 ± 0.167	2.057 ± 0.251	1.778 ± 0.084
	2.101	1.822 ± 0.112	1.904 ± 0.163	2.123 ± 0.254	1.837 ± 0.087
-0.317	2.101	1.821 ± 0.115	1.913 ± 0.296	2.156 ± 0.269	1.867 ± 0.084
	2.201	1.797 ± 0.115	1.892 ± 0.305	2.089 ± 0.267	1.807 ± 0.081
	2.101	1.818 ± 0.114	1.911 ± 0.296	2.155 ± 0.269	1.865 ± 0.084
-0.217	2.101	1.857 ± 0.086	1.946 ± 0.081	2.202 ± 0.34	1.872 ± 0.082
	2.201	1.833 ± 0.085	1.92 ± 0.079	2.13 ± 0.34	1.812 ± 0.079
	2.101	1.856 ± 0.085	1.945 ± 0.081	2.202 ± 0.34	1.87 ± 0.082
VL	VH_BLIND	M1	M2	M3	M4
-0.417	2.101	1.697 ± 0.133	1.684 ± 0.081	1.855 ± 0.084	1.819 ± 0.093
	2.201	1.654 ± 0.129	1.651 ± 0.077	1.838 ± 0.082	1.805 ± 0.092
	2.101	1.712 ± 0.134	1.697 ± 0.081	1.877 ± 0.086	1.84 ± 0.096
-0.317	2.101	1.746 ± 0.129	1.725 ± 0.064	1.895 ± 0.078	1.856 ± 0.086
	2.201	1.682 ± 0.128	1.677 ± 0.065	1.855 ± 0.074	1.82 ± 0.083
	2.101	1.742 ± 0.13	1.723 ± 0.065	1.89 ± 0.078	1.852 ± 0.086
-0.217	2.101	1.743 ± 0.08	1.725 ± 0.049	1.893 ± 0.074	1.842 ± 0.084
	2.201	1.683 ± 0.072	1.68 ± 0.05	1.855 ± 0.072	1.805 ± 0.078
	2.101	1.741 ± 0.079	1.723 ± 0.05	1.89 ± 0.074	1.84 ± 0.083

1342178914 Red (from Blue obs.)			
VL	VH_BLIND	M9	M10
-0.321	2.101	3.927 ± 0.285	4.146 ± 0.423
	2.202	3.887 ± 0.282	4.142 ± 0.423
	2.101	3.93 ± 0.285	4.151 ± 0.423
-0.221	2.101	3.874 ± 0.279	4.093 ± 0.433
	2.202	3.832 ± 0.276	4.085 ± 0.433
	2.101	3.875 ± 0.279	4.093 ± 0.433
-0.121	2.101	3.783 ± 0.344	3.922 ± 0.383
	2.202	3.722 ± 0.347	3.908 ± 0.388
	2.101	3.788 ± 0.342	3.924 ± 0.383

1342178914 Green					
VL	VH_BLIND	M5	M6	M7	M8
-0.417	2.101	1.184 ± 0.098	1.271 ± 0.178	1.53 ± 0.24	1.264 ± 0.07
	2.201	1.173 ± 0.099	1.263 ± 0.182	1.508 ± 0.243	1.242 ± 0.069
	2.101	1.192 ± 0.099	1.28 ± 0.179	1.54 ± 0.243	1.273 ± 0.069
-0.317	2.101	1.226 ± 0.102	1.323 ± 0.294	1.553 ± 0.259	1.284 ± 0.066
	2.201	1.205 ± 0.102	1.303 ± 0.3	1.52 ± 0.261	1.25 ± 0.065
	2.101	1.223 ± 0.102	1.32 ± 0.295	1.552 ± 0.259	1.28 ± 0.066
-0.217	2.101	1.256 ± 0.057	1.39 ± 0.481	1.528 ± 0.484	1.318 ± 0.064
	2.201	1.233 ± 0.058	1.373 ± 0.504	1.493 ± 0.518	1.285 ± 0.064
	2.101	1.255 ± 0.057	1.388 ± 0.481	1.53 ± 0.485	1.316 ± 0.064
VL	VH_BLIND	M1	M2	M3	M4
-0.417	2.101	1.153 ± 0.126	1.145 ± 0.066	1.337 ± 0.091	1.329 ± 0.098
	2.201	1.122 ± 0.121	1.106 ± 0.061	1.316 ± 0.089	1.31 ± 0.096
	2.101	1.163 ± 0.128	1.153 ± 0.067	1.355 ± 0.093	1.346 ± 0.1
-0.317	2.101	1.202 ± 0.122	1.181 ± 0.051	1.372 ± 0.081	1.363 ± 0.093
	2.201	1.141 ± 0.121	1.134 ± 0.05	1.332 ± 0.077	1.327 ± 0.09
	2.101	1.198 ± 0.123	1.179 ± 0.051	1.368 ± 0.081	1.359 ± 0.092
-0.217	2.101	1.189 ± 0.056	1.185 ± 0.034	1.369 ± 0.078	1.316 ± 0.079
	2.201	1.129 ± 0.052	1.139 ± 0.035	1.331 ± 0.076	1.281 ± 0.076
	2.101	1.187 ± 0.056	1.183 ± 0.035	1.369 ± 0.078	1.316 ± 0.08

1342178914 Red (from Green obs.)			
VL	VH_BLIND	M9	M10
-0.321	2.101	3.919 ± 0.282	4.149 ± 0.424
	2.202	3.879 ± 0.279	4.144 ± 0.423
	2.101	3.922 ± 0.282	4.152 ± 0.423
-0.221	2.101	3.867 ± 0.278	4.085 ± 0.431
	2.202	3.826 ± 0.275	4.078 ± 0.431
	2.101	3.871 ± 0.278	4.087 ± 0.431
-0.121	2.101	3.807 ± 0.344	3.92 ± 0.382
	2.202	3.75 ± 0.348	3.91 ± 0.387
	2.101	3.818 ± 0.343	3.926 ± 0.383

2.3 A flux gradient on the field of view?

RD6, which deals with the complete field of view scans performed on various orbits, demonstrates the existence of an illumination gradient in the field of view. This gradient is in the same direction for all filters, with more emission on the CS1 side, i.e. for the blue matrix 3, 4, 7, and 8 and the red matrix 9. The amplitude of the gradient in the central field of view is 100-150 ADU (B. Ali, private communication). The FOV scans are performed in low gain so 100 and 150 ADU convert to 2 mV and 3 mV respectively. To estimate how much flux this corresponds to we need the response and it is not yet known. However it should be in the range 2-4 10^{10} V/W, so the gradient in illumination is of the order of 0.05-0.15 pW/pix.

Looking at the tables above that list derived illuminations, we see also that the illumination does not appear to be flat but the story is more complex.

There is apparently more flux falling on the "right" side of the blue array (matrix 7, 8, 3, 4), with an offset amplitude of 0.1-0.2 pW/pix. Thus we could indeed be seeing the effect of the illumination gradient in the blue and green filter, although the amplitude we see is a bit larger than what the illumination gradient predicts.

On the red side we also see more flux, 0.1-0.2 pW/pix, on one side of the array but this time it is the "left" side that is brighter, matrix 10. This is incompatible with the brightness gradient seen in the FOV scan (note that this gradient is seen in the raw signal, i.e. it is independent from our flux conversion method). The only possible explanation is that the offset we see in our red flux tables comes from the method we use to convert the signal into flux and indicates the existence of a 0.2-0.4 pW/pix offset in the flux determination between matrix 10 and 9.

To be on the conservative side, the missmatch between the gradient amplitude and the left-right offset on the blue side is considered as an indication of a systematic uncertainty in the flux conversion method of $\sim$0.1 pW/pix for the blue and green filters.

3 OD 64 - Field of view scan on switched-off calibration sources

On OD 64, we performed a field-of-view scan dedicated to establish whether or not we had extra light on the red side of the photometer[1]. To this aim, the FOV scan was the first measurement of the period (after days of SPIRE and HIFI activities) and the switch-on of the instrument was performed with the calibration sources (CS1 and CS2) off. HK inspection shows that the resistor values are indeed 0.8 Ω, which corresponds to a temperature of 10 K (compared to a temperature of 55 K when they are nominally switched on). Given that for a black-body, a temperature of 10 K leads to a peak beyond the PACS red band, we expect a dramatic reduction of the flux measured on the CSs in all bands with respect to the nominal situation. The CSs are in fact very different from black-bodies and using our FM-ILT established calibration of their emission, we in fact expect no measurable flux in all photometer bands when looking at them cold.

A first indication that this is the case at least for the blue side comes from a simple plot of the raw signal measured during the scan as a function of chopper position (Figures 2, 3, and 4): for all the chopper positions where a matrix is looking at one of the calibration sources, we measure the same raw signal, whatever the calibration source and whatever the filter, blue or green.. The zoomed figures show that we have some variation of the measured raw signal from one scan to the other but thanks to the fact that we have forward and backward scans, we can verify that the variations in measured signal on the calibration sources are fully compatible with the known slowly variable offset drift that affects the bolometers. We unfortunately cannot make a similar analysis on the red channel as we only have a single filter there.

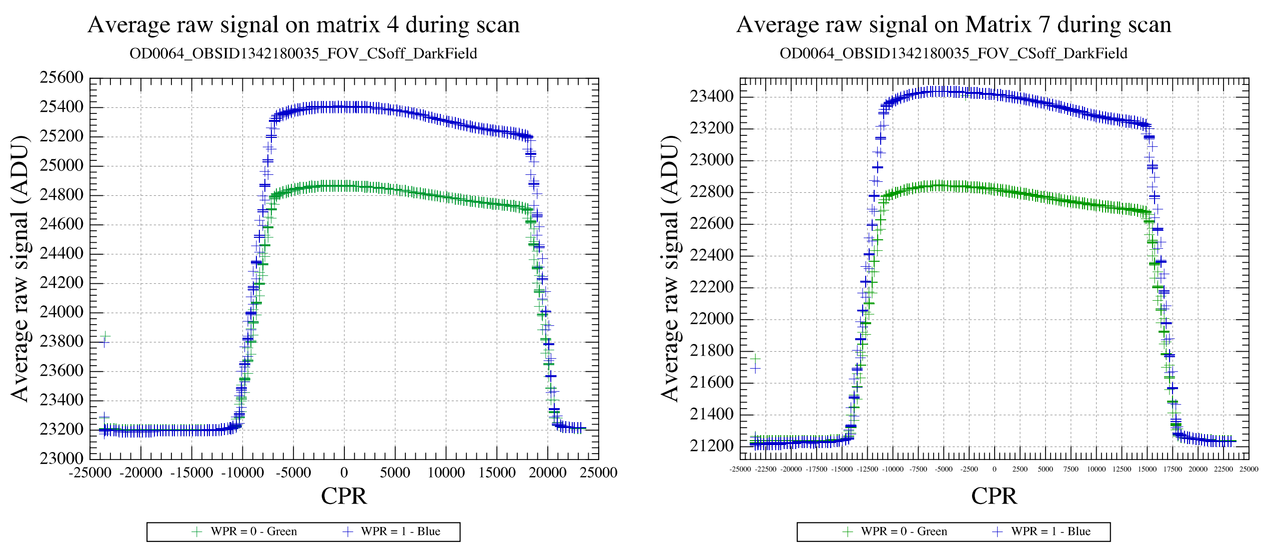

Figure 2: Average raw signal (ADU) measured on matrices 4 (left) and 7 (right) during the field of view scan as a function of chopper position (CPR). The green crosses show the green filter scan and the blue crosses the blue filter scan. As expected for a telescope temperature in the range of 80 K there is more flux in the blue filter than in the green filter, but when the matrices look at the two calibration sources, we see the same signal, whatever the source and whatever the filter (see also Figure 3 and 4 for a zoom on the calibration sources locations). The signal gradient on the open field-of-view mentioned in RD6 is clearly evident here and a similar plot for the red side confirms as well that a signal gradient with identical direction exists as well in the red.

This means both sources give the same output, and that the flux is the same in both filters. We can think of only two ways to produce this: either we have some flux on the blue side that is generated somewhere between

[1]On OD 46 we had already performed such a FOV scan with the calibration sources supposedly switched off. However this measurement is hard to use because: (1) the bias setting was not appropriate and a large number of pixels saturate on the calibration sources, (2) the calibration sources were switched off only 6 hr before the measurement when their cooling time is close to 12 hr, and (3) we discovered later on that the photometer switch on without the calibration sources actually commands them to 4.3 Ω where their temperature is around 23 K, i.e. already warm enough to produce flux in the red band.

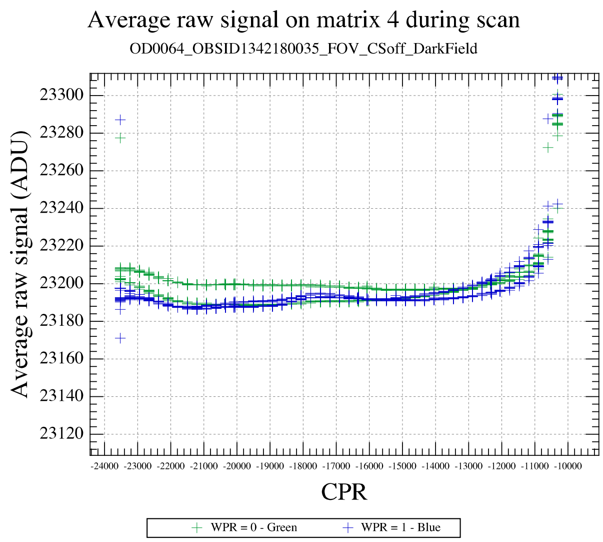

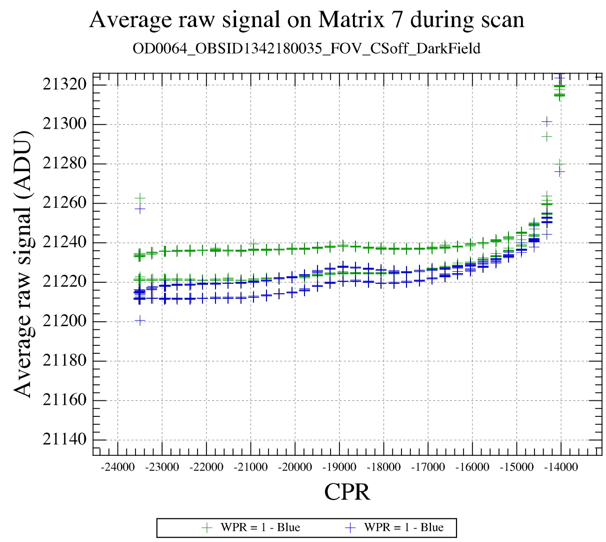

Figure 3: A zoom of Figure 2 on CS1 location (negative CPR). For each filter one clearly sees two "tracks" corresponding to the forward and backward scans. As the flux is very likely constant on the calibration source in a given filter, the offset between the two tracks can be interpreted as the offset drift. Then we clearly see that the difference in raw signal level between the green and the blue filter is fully compatible with the offset drift amplitude, and thus we are really seing the same flux level with both filters.

the detectors and the blue filter wheel (so as to have no filter dependence), and a check on the optical layout of PACS (RD7) shows that the only way to do that is to have emission coming from *inside* the blue photometer housing, or the signal that we observe on the blue side is 0 pW/pix (since a thermal source that would give similar non-zero blue and green flux would have a temperature in the range 30-40 K and we should have felt its presence in other ways...).

Let us now turn to a more quantitative analysis by converting the signal measured on the calibration sources into incoming fluxes.

The FOV-scan is a forward and backward scan of the complete field of view, defined by the extreme values that the chopper position can take, performed first in the green filter and then in the blue filter. From these scans, we extract the signal measured at the chopper position where the complete array is fully "illuminated" by the calibration sources. This is position −21200 for CS1 and +21270 for CS2 (these are not the standard calibration positions, rather a compromise between those defined as optimal from an inspection of previous FOV scans, see B. Ali's report, and the actually sampled positions). We checked on the raw signals that these positions are within 10-20 ADU s of the minimum signal recorded on the calibration sources for all matrices.

Given that these positions are not at the extreme of the chopper range, I can extract from the scan a series of short CS measurements. For the blue or green filter, I have two measurements per calibration sources as the scan passes each CS position twice: once forward and once backward. I note these Blue (or Green) CS1_1, CS1_2, CS2_1, and CS2_2. For the red filter, I have 4 measurements per CS and I refer to them with the same codes.

For each measurement I compute the mean image, and then convert it into a incoming flux using the two-stage interpolation as explained above. In the tables below I list, per matrix, the mean computed flux and the standard deviation per matrix. For each computation, the letter in parenthesis give the calibration set that was used to compute the flux.

The first striking aspect of these tables is that they are quite monotonous: whatever the configuration, we compute the same fluxes, which is a simple translation of the fact that when we look at a calibration source, CS1 or CS2, we see the same signal level. Furthermore, there is no clear difference between the green and blue values since, as mentioned before, we also get the same signal level in the two filters.

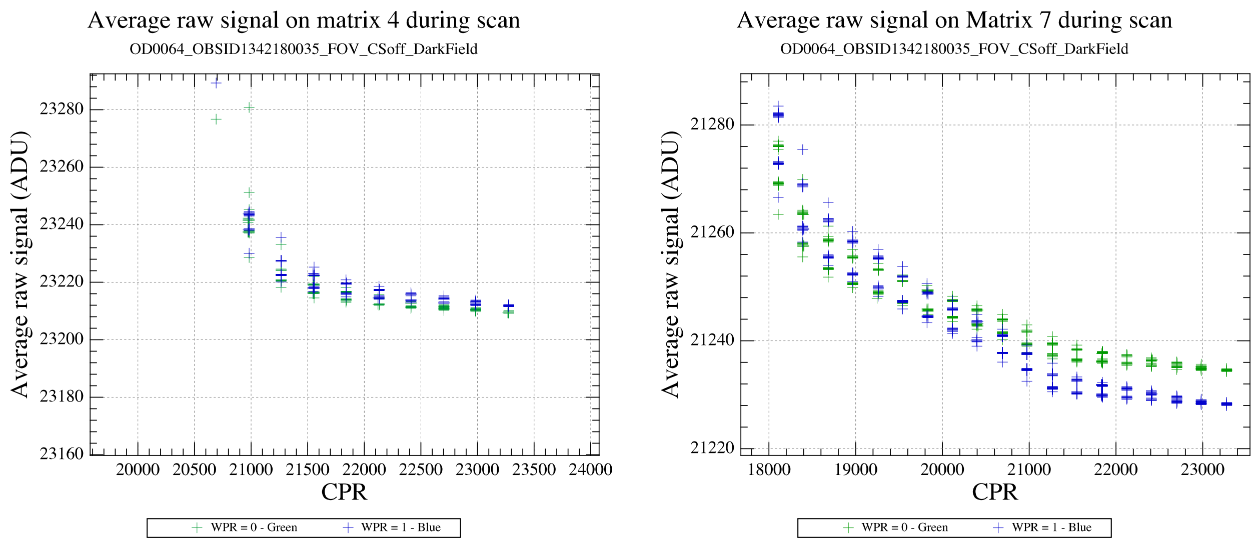

Figure 4: A zoom of Figure 2 on CS2 location (positive CPR). For each filter one clearly sees two "tracks" corresponding to the forward and backward scans. The same comments as those made for Figure 3 are valid here. Furthermore the signal level measured is compatible with the notion that we see the same flux level on both calibration sources.

OD0064_OBSID1342180035_FOV_CSoff Blue CS1_1					
VL	VH_BLIND	M5	M6	M7	M8
-0.397	2.163	0.131 ± 0.084 (B)	0.204 ± 0.085 (B)	0.413 ± 0.224 (B)	0.054 ± 0.088 (B)
VL	VH_BLIND	M1	M2	M3	M4
-0.397	2.163	0.078 ± 0.104 (B)	-0.002 ± 0.068 (B)	0.226 ± 0.122 (B)	0.201 ± 0.119 (B)

OD0064_OBSID1342180035_FOV_CSoff Red (from Blue CS1_1 obs.)			
VL	VH_BLIND	M9	M10
-0.346	2.185	1.52 ± 0.182 (R)	1.885 ± 0.392 (R)

OD0064_OBSID1342180035_FOV_CSoff Blue CS1_2					
VL	VH_BLIND	M5	M6	M7	M8
-0.398	2.163	0.114 ± 0.083 (B)	0.181 ± 0.083 (B)	0.395 ± 0.224 (B)	0.037 ± 0.086 (B)
VL	VH_BLIND	M1	M2	M3	M4
-0.398	2.163	0.087 ± 0.106 (B)	0.005 ± 0.068 (B)	0.199 ± 0.119 (B)	0.175 ± 0.118 (B)

OD0064_OBSID1342180035_FOV_CSoff Red (from Blue CS1_2 obs.)			
VL	VH_BLIND	M9	M10
-0.345	2.185	1.535 ± 0.183 (R)	1.911 ± 0.395 (R)

OD0064_OBSID1342180035_FOV_CSoff Blue CS2_1					
VL	VH_BLIND	M5	M6	M7	M8
-0.398	2.162	0.12 ± 0.081 (B)	0.203 ± 0.085 (B)	0.408 ± 0.223 (B)	0.068 ± 0.084 (B)
VL	VH_BLIND	M1	M2	M3	M4
-0.398	2.162	0.092 ± 0.107 (B)	0.019 ± 0.069 (B)	0.221 ± 0.12 (B)	0.209 ± 0.116 (B)

OD0064_OBSID1342180035_FOV_CSoff Red (from Blue CS2_1 obs.)			
VL	VH_BLIND	M9	M10
-0.345	2.185	1.564 ± 0.182 (R)	1.9 ± 0.388 (R)

OD0064_OBSID1342180035_FOV_CSoff Blue CS2_2					
VL	VH_BLIND	M5	M6	M7	M8
-0.397	2.162	0.16 ± 0.083 (B)	0.242 ± 0.087 (B)	0.457 ± 0.225 (B)	0.108 ± 0.087 (B)
VL	VH_BLIND	M1	M2	M3	M4
-0.397	2.162	0.084 ± 0.106 (B)	0.013 ± 0.07 (B)	0.257 ± 0.124 (B)	0.243 ± 0.12 (B)

OD0064_OBSID1342180035_FOV_CSoff Red (from Blue CS2_2 obs.)			
VL	VH_BLIND	M9	M10
-0.346	2.186	1.516 ± 0.179 (R)	1.849 ± 0.38 (R)

OD0064_OBSID1342180035_FOV_CSoff Green CS1_1					
VL	VH_BLIND	M5	M6	M7	M8
-0.397	2.162	0.158 ± 0.085 (B)	0.231 ± 0.086 (B)	0.438 ± 0.224 (B)	0.081 ± 0.089 (B)
VL	VH_BLIND	M1	M2	M3	M4
-0.397	2.162	0.126 ± 0.108 (B)	0.039 ± 0.071 (B)	0.233 ± 0.123 (B)	0.206 ± 0.118 (B)

OD0064_OBSID1342180035_FOV_CSoff Red (from Green CS1_1 obs.)			
VL	VH_BLIND	M9	M10
-0.345	2.185	1.516 ± 0.182 (R)	1.926 ± 0.398 (R)

OD0064_OBSID1342180035_FOV_CSoff Green CS1_2					
VL	VH_BLIND	M5	M6	M7	M8
-0.397	2.163	0.138 ± 0.084 (B)	0.206 ± 0.085 (B)	0.429 ± 0.225 (B)	0.069 ± 0.089 (B)
VL	VH_BLIND	M1	M2	M3	M4
-0.397	2.163	0.08 ± 0.105 (B)	-0.002 ± 0.069 (B)	0.234 ± 0.123 (B)	0.208 ± 0.12 (B)

OD0064_OBSID1342180035_FOV_CSoff Red (from Green CS1_2 obs.)			
VL	VH_BLIND	M9	M10
-0.346	2.185	1.512 ± 0.182 (R)	1.89 ± 0.392 (R)

OD0064_OBSID1342180035_FOV_CSoff Green CS2_1					
VL	VH_BLIND	M5	M6	M7	M8
-0.397	2.162	0.145 ± 0.083 (B)	0.227 ± 0.087 (B)	0.446 ± 0.224 (B)	0.1 ± 0.087 (B)
VL	VH_BLIND	M1	M2	M3	M4
-0.397	2.162	0.078 ± 0.106 (B)	0.005 ± 0.069 (B)	0.271 ± 0.127 (B)	0.254 ± 0.121 (B)

OD0064_OBSID1342180035_FOV_CSoff Red (from Green obs.)			
VL	VH_BLIND	M9	M10
-0.346	2.185	1.523 ± 0.18 (R)	1.862 ± 0.382 (R)

OD0064_OBSID1342180035_FOV_CSoff Green CS2_2					
VL	VH_BLIND	M5	M6	M7	M8
-0.397	2.163	0.129 ± 0.082 (B)	0.211 ± 0.086 (B)	0.421 ± 0.223 (B)	0.077 ± 0.085 (B)
VL	VH_BLIND	M1	M2	M3	M4
-0.397	2.163	0.103 ± 0.107 (B)	0.026 ± 0.07 (B)	0.226 ± 0.123 (B)	0.21 ± 0.117 (B)

OD0064_OBSID1342180035_FOV_CSoff Red (from Green CS2_2 obs.)			
VL	VH_BLIND	M9	M10
-0.345	2.185	1.548 ± 0.182 (R)	1.905 ± 0.388 (R)

Let us first concentrate on the blue side. We typically observe that some matrices appear to be getting no flux at all (e.g. the flux value computed is compatible with 0 given the dispersion for matrices 1, 2, 8), while another group would appear to give a marginal ($2\,\sigma$ at best for matrix 7) detection of a non-zero flux. Could this be real? We recall first that we identified the existence of a systematic flux conversion uncertainty of ∼0.1 pW/pix on the blue side. Considering this, it would appear that we have only one matrix, matrix 7, that could be measuring a non-zero flux. We however consider this quite unlikely: this matrix is physically surrounded by matrices that indicate a 0 pW/pix incoming flux (e.g. matrix 8). Furthermore we measure the same flux level in both filters (because we have the same raw signal in both filter). It becomes then extremely difficult to think that there could be a source of flux inside the blue bolometer housing that would only affect the flux on a single matrix.

Thus we think that the most probable conclusion is that we see no flux on the blue side, and as a future warning, we note that the conversion table for matrix 7 appears to overestimate the flux level by 0.3-0.4 pW/pix.

We are in a completely different situation on the red side where we do measure some flux when looking at the calibration sources, 1.5 to 1.9 pW/pix. We remark that the difference in the derived flux between matrix 9 and 10 has apparently increased when compared to the background measurement analysed in the previous section. This is fully understandable: when we look at the calibration sources, the illumination gradient present in the open field-of-view should be absent, thus revealing the full amplitude of the systematic uncertainty in the flux conversion method for the red side. This was estimated at 0.2-0.4 pW/pix. Therefore the numbers we get on the red side are quite compatible with a "flat" illumination of the array at a level around 1.5-1.9 pW/pix. This flux level is independent of the chopper position, i.e. we derive identical values whether we look at CS1 or CS2.

Thus the conclusion so far is that when we observe a dark source (i.e. a source that emits no flux in the photometer band), we indeed measure a signal corresponding to 0 pW/pix on the blue side of the photometer, but we measure a signal of 1.5-1.9 pW/pix on the red side of the photometer and this on each side of the open field-of-view, and thus presumably over the whole field of view.

Interestingly enough, we remark that the existence of a "flux offset" in the red band (due or not to an actual flux contribution, see below), assuming it has always been there with the same amplitude, would resolve a number of inconsistencies noted in the dedicated background measurements section: it is much easier to identify a telescope model that can reproduce the three band fluxes if we subtract ∼1.7 pW/pix to the red band fluxes, and we are also much more compatible with the simultaneous spectrometer background measurement in that case.

Let us know examine possible explanations.

4 Possible explanations and further tests

4.1 An error in the calibration tables

Given the complex process that we have to go through to get from a raw signal to the incoming flux, it is possible that an error has crept in the calibration tables. One painful way to check that would be to reprocess all the data that has been used to create them. This has been partially done. For the first part (the `VRL-VH_BLIND` calibration) we have extensively tested that nothing has changed significantly for the last 2.5 years, i.e. there

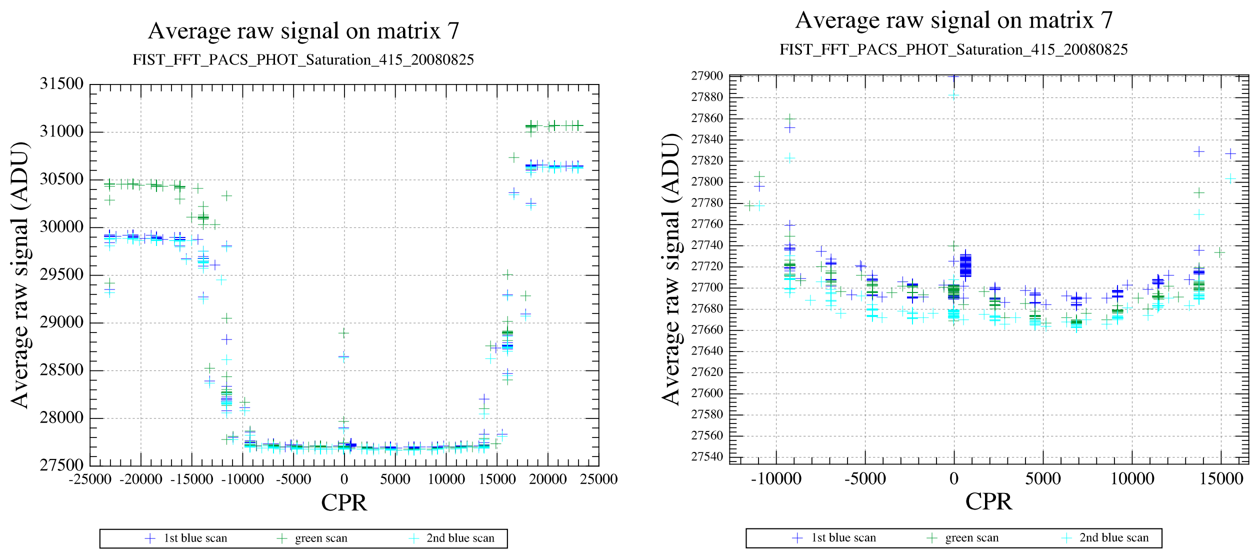

Figure 5: The average raw signal measured on He-flushed cryo-cover FOV scans on 20080825. Here the calibration sources are at their nominal settings. We see that they are both brighter in the green filter than in the blue filter which shows how different they are from a simple black-body (since their temperature is in the range 55-60 K). In the open field of view we see that the green scan gives the same raw signal value as the blue scans, again an indication that the flux there is close to 0 pW/pix.

FIST_FFT_PACS_PHOT_Saturation_415_20080825 Blue B1_1					
VL	VH_BLIND	M5	M6	M7	M8
-0.352	2.175	0.377 ± 0.063 (B)	0.385 ± 0.063 (B)	0.538 ± 0.103 (B)	0.37 ± 0.071 (B)
VL	VH_BLIND	M1	M2	M3	M4
-0.352	2.175	0.255 ± 0.962 (B)	0.256 ± 0.069 (B)	0.43 ± 0.101 (B)	0.427 ± 0.086 (B)

FIST_FFT_PACS_PHOT_Saturation_415_20080825 Red (from Blue B1_1 obs.)			
VL	VH_BLIND	M9	M10
-0.208	2.209	0.315 ± 0.085 (R)	0.209 ± 0.059 (R)

is full continuity between the measurements performed in the FM-ILT and those done in-flight. For the second part, the one linking V_{ptmil} to the incoming flux via the bolometer bias, we cannot make a test in-flight to check that it conforms with the FM-ILT measurement as we cannot absolutely control the incoming flux. However we have checked that reprocessing the FM-ILT data today gives the same results as those derived during the FM-ILT and stored in the calibration tables we use now.

Thus we are sure that there is no processing error in the calibration tables.

Furthermore we have interesting ground-based FOV-scans that were obtained during TV/TB (i.e. shortly before launch) with the cryo-cover flushed with Helium, i.e. rather dark (temperature around 15 K). For instance on August 25th, 2008, we performed the so-called saturation test, which consists of three fast FOV scans in blue, green and blue, on the crycover at 14.6 K. On Figure 5 we show the average raw signal on matrix 7 as a function of chopper position for the three scans.

From these scans we have extracted the data obtained when the chopper position is within $[-3000, +3000]$ which corresponds to the array looking at the open field of view. Since we have forward and backward scans again, and two scans in the blue filter, we obtain 4 independent background measurements in the blue filter, 2 in the green filter and 6 in the red filter. For brievity's sake, we only list the B1_1 and G_2 results (using the same naming principles as before).

FIST_FFT_PACS_PHOT_Saturation_415_20080825 Green G_2					
VL	VH_BLIND	M5	M6	M7	M8
-0.352	2.175	0.377 ± 0.063 (B)	0.383 ± 0.062 (B)	0.538 ± 0.109 (B)	0.372 ± 0.068 (B)
VL	VH_BLIND	M1	M2	M3	M4
-0.352	2.175	0.258 ± 0.963 (B)	0.251 ± 0.068 (B)	0.425 ± 0.1 (B)	0.422 ± 0.084 (B)

FIST_FFT_PACS_PHOT_Saturation_415_20080825 Red (from Green G_2 obs.)			
VL	VH_BLIND	M9	M10
-0.208	2.208	0.307 ± 0.086 (R)	0.215 ± 0.057 (R)

As expected, similar raw values in both blue and green filters lead to similar incoming flux values. However this time these values are rather homogenous (except notably for matrix 7) and not compatible with a 0 pW/pix flux. As mentioned before, if this flux was coming from a thermal source it would have a rather high temperature, but we have little reason to believe that looking inside the cryostat to the He-flushed cryo-cover would give us a black-body emission.

What is more important to point out here is the level of the emission on the red side, 0.2-0.3 pW/pix. Thus we can demonstrate with this observation that our conversion procedure is able to measure a low flux value on the red side (when we indeed expect one) and thus that it is unlikely that the reason we cannot measure a flux lower than 1.5 pW/pix in flight on the red side resides in the calibration tables used in the conversion procedure.

4.2 Stray-light in the instrument

If we assume that what we measure on the red side is an extra emission component, can it come from the instrument? We actually believe it is unlikely because:

- We have no indication that we see it on the blue side: (1) when the calibration sources are cold, we measure 0 pW/pix in the blue and green filters, (2) when we look at the sky we are compatible with the measurements made by the PACS spectrometer.
- It is rather independent of the chopper position, as indicated by the fact that the flux we measure on the cold calibration sources is of the same order as the flux we need to add to the spectrometer measurement to make it match our determination of the telescope background on the red side.
- The spectrometer is obviously not seeing this enhanced emission on either the red or the blue side.

So we would need to find a way to generate inside the instrument, but not on the spectrometer side, a significantly bright but very cold source. Again a look at the instrument's optical drawing shows that there is not much space to do that after the separation between photometer and spectrometer, and that space is so tight there that it is hard to understand how the blue side of the photometer could be completely immune.

4.3 A hot spot in the red bolometer housing

A possible way to generate a flux that is seen everywhere in the field of view but by only one side of the photometer is to have it inside the bolometer focal plane units. There are two electronics circuits there, namely the buffer units and the readout circuits, where a hot spot could form and generate flux. Since we are apparently operating with an excellent autonomy, it is unlikely that we have a hot spot at the 300 mK level as this would lead to increase dissipation. So a possible explanation is that we have a hot spot in one of the two buffer units of the red photometer. We can test that by performing observations with only one of the two red arrays switched on.

4.4 An effect of the detector temperature

Finally there's another way to modify the output of the bolometers, without flux, and it is to change the temperature of the focal plane. We have observed that if the temperature of the focal plane is lowered, then the position of V_{ptmil} will decrease, mimicking an higher flux level. This is an interesting possibility but we note that this requires a rather important change in the temperature (by more than 10 mK). Unfortunately we have no means of measuring the actual temperature on the focal plane so we cannot test whether the red bolometers are colder now than they were before.

Interestingly, if we switch on only one of the red arrays, this should further decrease the temperature of the red focal plane. If we indeed are seeing an effect of the focal plane temperature on the position of V_{ptmil} then we should measure more "flux" on the red side (as V_{ptmil} further decreases), while if what we see is an effect of a hot spot on one of the buffer units, we should see less flux.

5 Conclusions

Multiple lines of evidence point to the fact that we are effectively measuring more flux on the red side of the photometer compared to both what we could expect from a telescope model, and what we can extrapolate from the spectrometer measurements. The blue side of the photometer appears unaffected by this. Whether what we see is indeed more flux or an effect of a colder operating temperature of the red array remains to (and will) be tested.